

MEASUREMENTS OF THE POLARIZATION IN  $\pi^\pm p$  ELASTIC SCATTERING AT 5.15 GeV/c\*

R. J. Esterling,† N. E. Booth, G. Conforto, J. Parry, J. Scheid, and D. Sherden  
 The Enrico Fermi Institute and Department of Physics, The University of Chicago, Chicago, Illinois 60637

and

A. Yokosawa  
 Argonne National Laboratory, Argonne, Illinois 60439  
 (Received 2 October 1968)

We report results obtained at the zero-gradient synchrotron for the polarization in  $\pi^+p$  and  $\pi^-p$  elastic scattering at 5.15 GeV/c, from  $-t=0.2$  to 2.0 (GeV/c)<sup>2</sup>. The results may be qualitatively understood on the basis of a simple Regge-pole model. In addition to the flip amplitude due to  $\rho$  exchange, a significant  $I=0$  flip amplitude is required.

We have recently measured the polarization in  $\pi^\pm p$  elastic scattering at a laboratory momentum of 5.15 GeV/c over the range of  $-t=0.2$  to 2.0 (GeV/c)<sup>2</sup>. Previous measurements at high energies have been restricted to  $-t \lesssim 0.8$  (GeV/c)<sup>2</sup>.<sup>1</sup> The extended range of  $-t$  is important for testing Regge-pole models. In particular we can see what happens beyond  $t = -0.6$  (GeV/c)<sup>2</sup>, where  $\alpha_\rho(t) = 0$ .

The measurements were performed at the zero-gradient synchrotron (ZGS) with the Argonne polarized-proton target. Some of the experimental details have been briefly described before.<sup>2</sup> A seven-counter scintillation hodoscope in the incoming beam defined the pion momentum to  $\pm 0.5\%$  within a total acceptance of  $\pm 3.5\%$ . However, we found no significant change in polarization within the  $\pm 3.5\%$  interval so the data presented here are summed over the seven bins. Other hodoscopes in the beam measured the incident angle and position at which particles struck the polarized target. The  $\theta$  and  $\varphi$  angles and times of flight of both final-state particles were measured by means of arrays of scintillation counters. Events from  $\pi p$  scattering off the free protons of the lanthanum magnesium nitrate (LMN) target show up as peaks in the  $\theta$ -angular correlation of the two final-state particles. The background under the peaks was subtracted in two independent ways. One method was to use noncoplanar events to establish the shape of the  $\theta$  correlation for the background events. The second method was simply to interpolate the background under the peaks by fitting the events outside the peaks with a simple function. Both methods gave the same results well within errors. Incident beam intensities were typically  $10^6$  particles per pulse. The effective rate for the  $\pi^+$  measurements was less, since the beam composition was

75% protons and 25%  $\pi^+$ . Between 200 and 300 events per pulse were processed by an on-line computer. The computer immediately rejected those events with more than two final-state particles, made coplanarity and time-of-flight cuts, and sorted and stored the events for on-line display of various distributions, including the  $\theta$ -angular correlations. During each run the individual events were also written on magnetic tape, and at the end of each run the stored distributions were written on tape for subsequent analysis. Several NMR measurements of the target polarization were made during each run and processed by the computer at the end of the run. The value of  $-t$  and its resolution were determined for each counter which detected scattered pions by means of a Monte Carlo program which traced the incoming and scattered particles through the field of the polarized-target magnet.

The results for the polarization are shown in Fig. 1. The errors are statistical and include the uncertainty in background subtraction. There is an additional normalization error of  $\pm 10\%$  due to uncertainty in the target polarization which averaged about 0.55 over the duration of the experiment. The results are consistent with the behavior of the  $\pi^\pm p$  polarizations,  $P_\pm$ , which have been measured<sup>1</sup> for  $-t \lesssim 0.8$  at momenta between 6 and 12 GeV/c<sup>1</sup>; that is,  $P_+$  is positive while  $P_-$  is negative, and both become small near  $-t = 0.6$ . An interesting feature is that the maximum value of  $-P_-$  at small  $-t$  which is about 0.2 in Fig. 1 is essentially unchanged up to 12 GeV/c. On the other hand, the maximum value of  $P_+$  appears to decrease with increasing momentum.<sup>1</sup> Our results confirm that  $P_-$  goes positive in the region  $0.5 \lesssim -t \lesssim 0.8$  as is suggested by the earlier results at 6 GeV/c.<sup>1</sup> Note that  $P_+$  does not, in a corresponding way, become negative in this in-

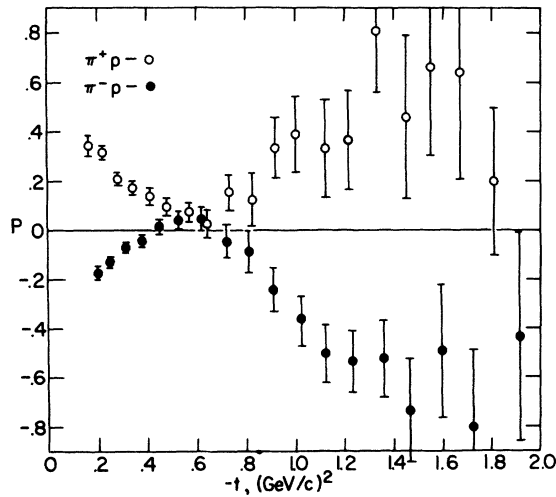


FIG. 1. Polarization in  $\pi^\pm p$  elastic scattering at 5.15 GeV/c.

terval, but is closely equal to  $P_-$ . In our preliminary data at lower momenta  $P_+ \approx P_-$  near  $-t = 0.6$  to a remarkable degree while the magnitude of  $P_\pm$  is as large as 0.15 and clearly inconsistent with zero. At larger values of  $-t$ ,  $P_+$  and  $P_-$  diverge again, with  $P_+$  remaining positive and  $P_-$  becoming again negative.

Polarizations and other experimental data at high energies have been fitted by a series of Regge-pole models.<sup>3-5</sup> In these models the  $I=0$  exchange amplitude consists of the Pomanchuk ( $P$ ) and the  $P'$  Regge poles. For the  $I=1$  exchange amplitude, the  $\rho$  Regge pole is used. In these models the dominant polarization term at small  $-t$  comes from the real part of the flip amplitude of the  $\rho$  trajectory interfering with the imaginary part of the nonflip amplitude of the  $P$  and  $P'$ . Because the  $I=1$   $\rho$  trajectory contributes with opposite sign to the  $\pi^+ p$  and  $\pi^- p$  amplitudes and the  $I=0$  trajectories contribute with the same sign, we have<sup>6</sup>

$$P_\pm(t) \approx \pm \frac{\sin\theta \operatorname{Im}[A_0'(t)B_1^*(t)]}{16\pi\sqrt{s} \frac{d\sigma}{dt}_\pm} \approx \pm \frac{\sin\theta \operatorname{Im}A_0'(t) \operatorname{Re}B_\rho(t)}{16\pi\sqrt{s} \frac{d\sigma}{dt}_\pm}, \quad (1)$$

where<sup>7</sup>

$$\operatorname{Re}B_\rho(t) \propto \alpha_\rho(t) \tan\left[\frac{1}{2}\pi\alpha_\rho(t)\right] / \Gamma(\alpha_\rho(t) + 1). \quad (2)$$

Thus to first order,  $P_-(t) = -P_+(t)$  and both vanish at  $\alpha_\rho(t) = 0$  which occurs at  $-t \approx 0.6$ .<sup>8</sup> The models differ considerably in their predictions

beyond  $-t = 0.6$ ,<sup>9</sup> and only one of them has attempted to fit data beyond  $-t = 1.0$  (GeV/c)<sup>2</sup>.<sup>4</sup> Our data show that  $P_-(t) \approx P_+(t)$  at large  $-t$  as well, indicating that the  $\rho$  still dominates the polarization at values of  $-t$  well beyond 0.6. Note that when  $\alpha_\rho(t)$  passes through zero, both factors in the numerator of Eq. (2) change sign. Thus,  $P_+$  stays positive and  $P_-$  negative, provided  $\operatorname{Im}A_0'(t)$  does not also change sign.

Within the framework of the three-pole model,  $\operatorname{Im}A_0'(t) \approx \operatorname{Im}A_{P'}(t)$  at small  $-t$ . However, at the larger values of  $-t$  [say between 1 and 2 (GeV/c)<sup>2</sup>], the elastic cross sections decrease rapidly with increasing energy. This indicates that  $\operatorname{Im}A_0'(t) \approx \operatorname{Im}A_{P'}(t)$ .<sup>4</sup> For Eqs. (1) and (2) to work we need to ensure that  $\operatorname{Im}[A_{P'}(t) + A_{P''}(t)]$  remains positive beyond  $-t \approx 0.6$ . Since, very likely,  $\alpha_{P'}(t)$  passes through zero somewhere near  $-t = 0.6$ ,<sup>10</sup> it may be important to consider what happens to  $\operatorname{Im}A_{P'}(t)$  at  $\alpha_{P'}(t) = 0$ . In most of the Regge fits a factor of  $\alpha_{P'}$  is used to eliminate the pole in  $\operatorname{Re}A_{P'}(t)$  and this makes  $\operatorname{Im}A_{P'}(t)$  change sign.<sup>3,5</sup> The no-compensation mechanism (factor of  $\alpha_{P'}^2$ ), on the other hand, maintains the same sign.<sup>4</sup> Although other explanations are no doubt possible, these simple considerations tend to favor no sign change in  $\operatorname{Im}A_{P'}(t)$ .<sup>11</sup>

To the extent that  $P_-(t) \neq -P_+(t)$ , one must introduce terms of the type  $A_0'B_0^*$  which appear symmetrically in  $P_+$  and  $P_-$ . This may also allow  $P_+$  to decrease with increasing momentum while holding  $P_-$  approximately constant. The above-mentioned models have not been particularly successful in duplicating this aspect of the data.<sup>12</sup>

The relative roles of the terms which are symmetric and antisymmetric with respect to  $\pi^+ p$  and  $\pi^- p$  are illustrated in Fig. 2. There we have plotted the combinations

$$\frac{1}{\sin\theta} \left[ \left( P \frac{d\sigma}{dt} \right)_+ - \left( P \frac{d\sigma}{dt} \right)_- \right] = \frac{1}{8\pi\sqrt{s}} [\operatorname{Im}(A_0'B_1^*) + \operatorname{Im}(A_1'B_0^*)], \quad (3)$$

and<sup>13</sup>

$$\frac{1}{\sin\theta} \left[ \left( P \frac{d\sigma}{dt} \right)_+ + \left( P \frac{d\sigma}{dt} \right)_- \right] = -\frac{1}{8\pi\sqrt{s}} [\operatorname{Im}(A_0'B_0^*) + \operatorname{Im}(A_1'B_1^*)]. \quad (4)$$

The second term on the right-hand side of Eq. (4) is equal to  $(Pd\sigma/dt)_0/\sin\theta$ , the polarized charge-exchange cross section divided by  $\sin\theta$ .

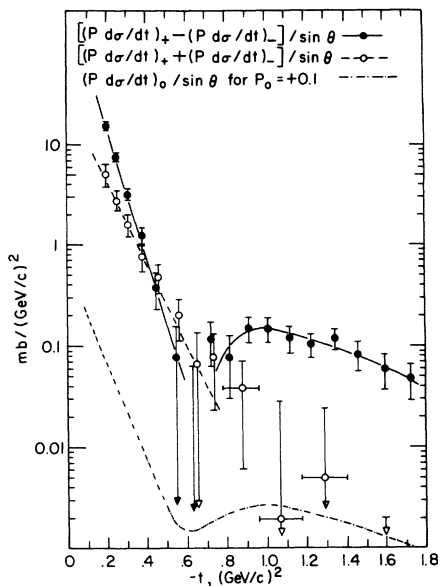


FIG. 2. Plots of  $(\sin\theta)^{-1}[(P d\sigma/dt)_+ \pm (P d\sigma/dt)_-]$  derived from the data of Fig. 1. Also shown is  $(\sin\theta)^{-1} \times (P d\sigma/dt)_0$  calculated from the charge exchange cross section and the assumption that  $P_0 = +0.1$ .

In the simple three-pole model this is identically zero. However, experimentally  $P_0 \approx 0.1$  for  $-t < 0.4$ .<sup>14</sup> Even so,  $\text{Im}(A_1'B_1^*)$  is negligible compared with  $\text{Im}(A_0'B_0^*)$  for  $-t \leq 0.4$  where measurements of  $P_0$  have been made. Possibly  $P_0$  is even larger at larger values of  $-t$ , but only for  $-t \gtrsim 0.8$  could  $\text{Im}(A_1'B_1^*)$  become comparable with  $\text{Im}(A_0'B_0^*)$ . For completeness we have also plotted  $(P d\sigma/dt)_0/\sin\theta$  in Fig. 2 assuming  $P_0 = +0.1$  at all  $t$ .

The dramatic behavior of the antisymmetric combination [Eq. (3)] shown in Fig. 2 is consistent with the vanishing of  $B_\rho(t)$  at  $\alpha_\rho(t) = 0$ . Also  $\text{Im}[A_1'B_0^*]$  appears to be negligible at least at  $-t \approx 0.6$ . On the other hand, the symmetric combination [Eq. (4)] appears to fall off smoothly with increasing  $-t$ .

Since both sets of points in Fig. 2 appear to exhibit exponential behavior at small  $-t$ , we have fitted them with the function  $Ae^{bt}$  which is often used to fit differential cross sections. The results are shown in Table I. The slopes are steeper than the value  $8 (\text{GeV}/c)^{-2}$  obtained for  $(d\sigma/dt)_\pm$  at momenta near  $5 \text{ GeV}/c$ .<sup>15</sup>

In the three-pole model the symmetric combination in Fig. 2 is due to interference between the  $P$  and  $P'$  trajectories. We have seen previously that the no-compensation mechanism for the  $P'$  provided an attractive explanation for the sign of the antisymmetric combination at large  $-t$ . How-

Table I. Results of fitting  $[(P d\sigma/dt)_+ \pm (P d\sigma/dt)_-]/\sin\theta$  with  $Ae^{bt}$ .

Combination	Range of fit [ $(\text{GeV}/c)^2$ ]	A [ $\text{mb}/(\text{GeV}/c)^2$ ]	b [ $(\text{GeV}/c)^{-2}$ ]
Antisymmetric [Eq. (3)]	$-t \leq 0.6$	$282 \pm 61$	$14.4 \pm 0.8$
Symmetric [Eq. (4)]	$-t \leq 0.8$	$29 \pm 10$	$9.25 \pm 1.0$
Symmetric [Eq. (4)]	$-t \leq 1.8$	$28 \pm 10$	$9.1 \pm 1.0$

ever, this mechanism makes both  $AP'$  and  $BP'$  vanish at  $\alpha_{P'} = 0$ . Then, except for the small contribution of  $\text{Im}(A_1'B_1^*)$ , the symmetric combination vanishes at  $\alpha_{P'} = 0$ . This does not appear to be supported by the data. Although other explanations within the framework of the three-pole model may be possible, the nonzero charge-exchange polarization data<sup>14</sup> point out obvious limitations of the simple model.

We sincerely thank the many members of the Enrico Fermi Institute and of the Particle Accelerator Division, High Energy Physics Division, and High Energy Facilities Division of Argonne National Laboratory for their assistance and cooperation.

\*Work supported by the National Science Foundation under Grant No. GP-6135 (with some assistance from Grant No. GU-2175) and in part by the U. S. Atomic Energy Commission.

†Present address: Physics Department, Rutgers, The State University, New Brunswick, New Jersey.

<sup>1</sup>M. Borghini, G. Coignet, L. Dick, D. Kuroda, L. diLella, P. C. Macq, A. Michalowicz, and J. C. Oliver, Phys. Letters **24B**, 77 (1967). New measurements of the polarization in  $\pi^+p$  scattering at  $14 \text{ GeV}/c$  have also been made. See R. T. Bell, M. Borghini, L. Dick, G. Gregoire, L. diLella, J. C. Oliver, M. Poulet, P. Scharff-Hansen, D. Cronenberger, K. Kuroda, A. Michalowicz, G. Bellettini, P. L. Braccini, T. Del Prete, L. Foa, G. Sanguinetti, and M. Valdata, in Proceedings of the Fourteenth International Conference on High Energy Physics, Vienna, 1968 (to be published).

<sup>2</sup>N. E. Booth, G. Conforto, R. J. Esterling, J. Parry, J. Scheid, D. Sherden, and A. Yokosawa, Phys. Rev. Letters **21**, 651 (1968).

<sup>3</sup>C. B. Chiu, R. J. N. Phillips, and W. Rarita, Phys. Rev. **153**, 1485 (1967).

<sup>4</sup>C. B. Chiu, S. Y. Chu, and L. L. Wang, Phys. Rev. **161**, 1563 (1967).

<sup>5</sup>W. Rarita, R. J. Riddell, Jr., C. B. Chiu, and R. J. N. Phillips, Phys. Rev. **165**, 1615 (1968).

<sup>6</sup>We use the notation of V. Singh, Phys. Rev. **129**, 1889 (1963), except we use  $A_0', A_1'$  for his  $A'^{(+)}, A'^{(-)}$ ,

etc.

<sup>7</sup>See for example, C. Schmid, Phys. Rev. Letters 20, 689 (1968); G. Höhler, J. Baacke, and G. Eisenbeiss, Phys. Letters 22, 203 (1966).

<sup>8</sup>G. Höhler, J. Baacke, H. Schlaile, and P. Sonderegger, Phys. Letters 20, 79 (1966).

<sup>9</sup>Although beyond  $-t \approx 1.0$  (GeV/c)<sup>2</sup>, only solution (b) of Ref. 3 disagrees strongly with our polarization data, only the fit of Ref. 4 is also consistent with the differential cross-section data at large  $-t$ .

<sup>10</sup>N. E. Booth, Phys. Rev. Letters 21, 465 (1968).

<sup>11</sup>A double sign change may also be possible. See F. J. Gilman, H. Harari, and Y. Zarmi, Phys. Rev.

Letters 21, 323 (1968).

<sup>12</sup>In Ref. 4 the  $P$  and  $P'$  flip amplitudes were neglected so  $A_0' B_0^*$  is necessarily zero.

<sup>13</sup>Since complete elastic cross-section data are not yet available at this momentum we have used values of  $(d\sigma/dt)_\pm$  and  $(d\sigma/dt)_0$  calculated from the Regge-pole model of Ref. 4. This model fits cross-section data between 3 and 10 GeV/c fairly well, at least out to  $-t = 1.5$ .

<sup>14</sup>D. Drobnis *et al.*, Phys. Rev. Letters 20, 274 (1968); P. Bonamy *et al.*, Phys. Letters 23, 501 (1966).

<sup>15</sup>See for example, C. C. Ting, L. W. Jones, and M. L. Perl, Phys. Rev. Letters 9, 468 (1962).

PARTIAL-WAVE ANALYSIS OF THE SEQUENTIAL REACTION  $K^-N \rightarrow Y_1^*(1385)\pi \rightarrow \Lambda\pi\pi$   
IN THE CENTER-OF-MASS ENERGY RANGE 1600-1740 MeV\*

W. H. Sims, J. R. Albright, E. B. Brucker, J. T. Dockery,† J. E. Lannutti,  
J. S. O'Neall,‡ and B. G. Reynolds  
The Florida State University, Tallahassee, Florida

and

J. H. Bartley, R. M. Dowd, A. F. Greene,§ and J. Schneps  
Tufts University, Medford, Massachusetts

and

M. Meer,|| J. Mueller, M. Schneeberger, and S. Wolf  
Brandeis University, Waltham, Massachusetts  
(Received 3 September 1968)

The reaction  $K^-n \rightarrow \Lambda\pi^-\pi^0$  for c.m. energies from 1600 to 1740 MeV is found to proceed entirely through the two-body  $Y_1^*(1385)\pi$  state. A partial-wave analysis of the  $Y_1^*(1385)\pi$  state implies  $s$ -channel production of  $Y_1^*(1660)$ ,  $Y_1^*(1765)$ , and a  $Y_1^*(1700)$  with the subsequent decay of each into  $Y_1^*(1385)\pi$ . A determination of the mass, width, elasticity parameter, spin, and parity of each of these  $s$ -channel resonant states has been made.

The analysis discussed in this Letter considers, in a formation experiment, the pure  $I=1$   $\Lambda\pi\pi$  final state and the sequential decay  $Y^* \rightarrow \Sigma(1385)\pi \rightarrow \Lambda\pi\pi$ . This assumed sequential decay offers certain advantages for analysis since if a resonant state decays through the  $\Sigma(1385)$  which has spin  $\frac{3}{2}$ , and a  $\pi$  which has spin 0, then the production angular distribution of the  $\Sigma(1385)$  will be free of the Minami ambiguity and will, in principle, uniquely determine the spin and parity  $J^P$  of the parent resonant state.<sup>1</sup> However, in this energy region, interference effects and overlapping  $\Sigma(1385)$  bands are expected to distort this and other distributions<sup>2</sup> as either pion may form a  $\Sigma(1385)$  with the lambda and Bose statistics are required for the final-state pions. Since direct  $s$ -channel production is believed to dominate the  $\Sigma(1385)\pi$  state at

this energy,<sup>3</sup> a partial-wave analysis is feasible provided the distorting effects mentioned above are taken into account. The isobar-model formulation of Deler and Valladas,<sup>4</sup> hereinafter referred to as DV, accounts for these effects and is used in the following partial-wave analysis.

The experimental data for this analysis were obtained from an exposure of the Brookhaven National Laboratory 30-in. deuterium-filled bubble chamber to  $K^-$  beams of momenta 670, 720, 770, 810, 850, and 910 MeV/c. The reaction analyzed was  $K^-n(p) \rightarrow \Lambda\pi^-\pi^0(p)$ , where ( $p$ ) indicates the spectator proton. Fits were accepted only for those events having a measurable spectator proton, and a  $\chi^2$  probability  $\geq 5\%$ . Events accepted in this analysis also were required to have a spectator momentum less than 280 MeV/c. The spectator-momentum distribution of